Oxidation of *aci*-Nitromethane by Singlet Oxygen in Aqueous Solution

Piotr Bilski,* Krzysztof Reszka, and Colin F. Chignell

Contribution from Laboratory of Molecular Biophysics, National Institute of Environmental Health Sciences, Research Triangle Park, North Carolina 27709

Received May 20, 1994®

Abstract: In alkaline solution nitromethane (NM) forms a stable *aci* tautomer ($H_2C{=}NO_2^-$) which may be used as a spin trap for radicals, including NO• and NO_2•. We have noticed previously that in aerated photochemical systems NM can undergo photosensitized degradation (Bilski *et al.*, *J. Am. Chem. Soc.* **1992**, *114*, 549), possibly *via* singlet oxygen ($^1O_2$). We have now confirmed that *aci*-NM does indeed quench $^1O_2$ phosphorescence ($k_q = 2.4 \times 10^7$ M^{-1} s^{-1}), and that the addition of $^1O_2$ to *aci*-NM is solely responsible for this chemical quenching, as confirmed by the high quantum yield of O_2 photoconsumption ($\phi = 0.65$ for [NM] = 35 mM). To obtain "labeled" fragments from the decomposition of the resultant *aci*-NM–O_2 peroxy species we have applied another spin trap, 5,5-dimethyl-1-pyrroline *N*-oxide (DMPO), in a novel way: we used an EPR silent hydroxylamine adduct (DMPOH/$CH{=}NO_2^-$) formed by nucleophilic addition of *aci*-NM to DMPO. Reaction of DMPOH/$CH{=}NO_2^-$ with $^1O_2$ resulted in the generation of the DMPO/$CO_2^{\bullet-}$ radical, suggesting that in the absence of DMPO the following mechanism may occur: $^1O_2 + CH_2{=}NO_2^- \rightarrow NO_2^- + HCOOH$. We have found that nitrite and formate production accounts for most of the oxygen consumed. This suggests that $^1O_2$ reacts mainly with the carbon atom of NM producing a biradical transient which decomposes yielding thermodynamically stable products nitrite and formate. A minor product is peroxynitrite ($OONO^-$) which must be produced *via* an ozonide-type intermediate formed by intramolecular recombination of the biradical. Prolonged irradiation of Rose Bengal and *aci*-NM resulted in accumulation of nitrite which was then photooxidized to NO_2•, trapped by unreacted *aci*-NM and identified as the NM/NO_2• spin adduct.

Introduction

The *aci* tautomer of nitromethane ($H_2C{=}NO_2^-$) contains a double bond which is stabilized by proton dissociation (pK = 10.2 for the nitro form).[1] The unsaturated character of the *aci* form has been used for trapping various free radical species.[2-4] Nitromethane has proved to be particularly useful for the identification of nitrogen-centered radicals[4,5] such as NO_2• and NO•, which do not form stable adducts with nitrone and nitroso spin-trapping agents. Such nitrogen-centered radicals are involved in many processes of biological[6-10] and environmental[11-13] interest.

Because spin trapping is an integrating method, a spin trap like *aci*-nitromethane may often be used for relatively long time periods in order to produce detectable radical (spin adduct) concentrations. Under these conditions side reactions involving the spin trap may interfere with spin trapping efficacy, or may generate radical species not related to the process under investigation. These side reactions must be understood if the reaction of interest is to be interpreted correctly.

When the spin trap NM is employed to identify radicals produced during photooxidation, the main oxidizer is frequently singlet oxygen, and even with other oxidizers, singlet oxygen is often concomitantly generated as a side product. The possibility that *aci*-NM may react with $^1O_2$ was suggested when we observed that NM was degraded during use as a spin trap in the UV photolysis of nitrite anion,[4] which generated traces of $^1O_2$. It is known that $^1O_2$ can oxidize >C=N double bonds in oximes, hydrazones or nitrones,[14-16] thus the unsaturated character of the *aci*-NM anion may make it a good $^1O_2$ substrate.

In the present work we have studied the reaction between *aci*-NM and $^1O_2$ generated by visible light irradiation of Rose Bengal. We have found that $^1O_2$ is chemically quenched by *aci*-NM, resulting in NM degradation, oxygen consumption and the production of nitrite and formate anions. We have also developed a novel application of the spin trap DMPO to elucidate the photooxidation mechanism for this reaction.

Experimental Section

Rose Bengal, nitromethane (99% purity), NaOH (semiconductor grade), 5,5-dimethyl-1-pyrroline *N*-oxide (DMPO), diethylenetriaminepentaacetic acid (DTPA), *N*-(1-naphthyl)ethylenediamine dihydrochloride, and sulfanilamide were purchased from Aldrich Chemical Co. Milwaukee, WI. DMPO was vacuum distilled and stored at -40 °C. Buffers were prepared from reagent grade or better components, and pH was measured using a glass electrode. The preparation of micellar and nonmicellar solutions of RB was described previously.[17]

In some experiments we used RB sequestered in negatively charged micelles to eliminate potential quenching of the RB triplet by the *aci*-NM anion and because micellar RB is more photostable.[17] However, because we did not observe any essential differences between photosensitization in micellar and nonmicellar solution, the results from micellar solution are not presented.

Absorption spectra were recorded on a HP 8451-A diode array spectrophotometer (Hewlett-Packard Instrument Co., Palo Alto, CA). EPR spectra were recorded on a Varian E-Line Century Series (Palo Alto, CA) spectrometer as previously described.[18a] Irradiations for EPR experiments were carried in a quartz EPR flat cell using a TM_{110} cavity.

* Abstract published in *Advance ACS Abstracts*, October 1, 1994.

(1) Turnbull, D.; Maron, S. H. *J. Am. Chem. Soc.* **1943**, *65*, 212.
(2) Behar, D.; Fessenden, R. W. *J. Phys. Chem.* **1972**, *76*, 1710.
(3) Gilbert, B. C.; Norman, R. O. C. *Can. J. Chem.* **1982**, *60*, 1379.
(4) Bilski, P.; Chignell, C. F.; Szychlinski, J.; Borkowski, A.; Oleksy, E.; Reszka, K. *J. Am. Chem. Soc.* **1992**, *114*, 549.
(5) Reszka, K.; Chignell, C. F.; Bilski, P. *J. Am. Chem. Soc.* **1994**, *116*, 4119.
(6) Henry, Y.; Ducrocq, C.; Drapier, J.-C.; Servent, D.; Pellat, C.; Guissani, A. *Eur. Biophys. J.* **1991**, *20*, 1.
(7) Snyder, S. H. *Science* **1992**, *257*, 494.
(8) Stamler, J. S.; Singel, D. J.; Loscalzo, J. *Science* **1992**, *258*, 1898.
(9) Traylor, T. G.; Sharma, V. S. *Biochemistry*, **1992**, *31*, 2847.
(10) Schmidt, H. H. H. W. *FEBS Lett.* **1992**, *307*, 102.
(11) Baumgärtner, M.; Conrad, R. *FEMS Microbiol. Ecol.* **1992**, *101*, 59.
(12) Elstner, E. F.; Oßwald, W. *Free Radical Res. Commun.* **1991**, *12-13*, 795.
(13) Wayne, R. P.; Barnes, I.; Biggs, P.; Burrows, J. P.; Canosa-Mas, C. E.; Hjorth, J.; Le Bras, G.; Moortgat, G. K.; Perner, D.; Poulet, G.; Restelli, G.; Sidebottom, H. *Atmos. Environ.* **1991**, *25A*, 1, and references therein.
(14) Castro, C.; Dixon, M.; Erden, I.; Ergonenc, P.; Keeffe, J. R.; Sukhovitsky, A. *J. Org. Chem.* **1989**, *54*, 3732, and references therein.
(15) Erden, I.; Griffin, A.; Keeffe, J. R.; Brinck-Kohn, V. *Tetrahedron Lett.* **1993**, *34*, 793-796.
(16) (a) Williams, J. R.; Unger, L. R.; Moore, R. H. *J. Org. Chem.* **1978**, *43*, 1271. (b) Yamashita, M.; Nomoto, H.; Imoto, H. *Synthesis* **1987**, 716.

Singet oxygen lifetimes in solution were measured using a laser flash photolysis spectrometer which will be described in detail elsewhere.[18b] Briefly, the apparatus utilized a MY-33 Nd:YAG laser (Laser Photonics, Orlando, FL) and a germanium diode (Model 403 HS, Applied Detector Corporation, Fresno, CA) in conjunction with an appropriate optical system. The $^1O_2$ lifetimes calculated from exponential decays were 54.5 μs in D_2O and 4.4 μs in H_2O, which agree well with most published values. The high sensitivity of this instrumentation allowed us to measure $^1O_2$ lifetime after a single pulse of excitation without resorting to multipulse averaging with a flow system.

Previously described methods were used to measure oxygen photoconsumption and to measure actinometrically the quantum yield of NM oxidation.[18] For solutions containing RB, the exciting light was passed through a combination of glass cutoff filters (450 nm) and neutral filters to attenuate the light intensity (usually about 60 times). Under such conditions RB photobleaching was negligible. The system for monitoring steady-state singlet oxygen phosphorescence has been described.[19] During steady-state phosphorescence measurements oxygen was bubbled through the sample to compensate for oxygen photoconsumption.

The stoichiometry of photoconsumed oxygen relative to oxidized NM was measured as follows: A solution containing NaOH (0.25 M) and RB (50 μM) was saturated with oxygen at 25 °C until the signal from the oxygen electrode remained constant. The oxygen concentration (1.14 mM) was calculated using O_2 solubility in water[20] taking into account the salting-out coefficient of 0.18 for O_2 in 0.25 M NaOH.[21] To this sample we added NM (0.5 mM) and then irradiated for ca. 0.5 h until O_2 consumption had practically ceased. At this stage, all NM and its oxidizable degradation products were oxidized. Oxygen consumption due to RB photobleaching was measured in the absence of NM and then subtracted from the photochemical effect. During the stoichiometric measurements RB was strongly bleached by the *aci*-NM photooxidation products.

Nitrite anion was assayed by adapting a sensitive spectrophotometric method based on the coupling of diazotized sulfanilamide with *N*-(1-naphthyl)ethylenediamine dihydrochloride.[22] This assay must be performed at pH 1, which has the advantage that RB loses its red color due to lactamization, so that the photosensitizer does not interfere with the azo dye assay at 543 nm. On the other hand, there is the disadvantage that at acidic pH values NO_2^- and *aci*-NM react to yield pseudonitroles.[23a] (During acidification of the irradiated sample, nitronate anion, $CH_2{=}NO_2^-$, is converted to nitronic acid, $CH_2{=}NO_2H$, (pK_a^{aci} = 3.25),[23a] and NO_2^- to nitrous acid (pK = 3.28)[23b]). In addition, when sulfanilamide was present during acidification, diazonium compounds formed from the reaction of this sulfanilamide and nitrous acid also reacted with the nitronic acid, probably forming nitroaldehyde hydrazone;[23a] such a reaction was suggested by the appearance of a yellow color during acidification (λ_{max} = 430 nm, not shown). Thus, the concentrations of both nitrite and diazonium intermediate available for coupling with the *N*-(1-naphthyl)ethylenediamine tended to be seriously reduced due to these side reactions.

To overcome the above analytical problems in the assay of nitrite, irradiations were performed using low concentrations of *aci*-NM. These concentrations were determined both by pH and added NM. Irradiation time was adjusted so that only about 30% of the oxygen was depleted. Irradiated alkaline samples were neutralized before further analysis with NaH_2PO_4 (0.5 M), which allowed the tautomerization of unreacted $CH_2{=}NO_2H$ to CH_3NO_2 (k = 4.1 × 10^4 M^{-1} min^{-1})[23a] to occur; nitromethane in its nitro form did not interfere with the nitrite analysis. (During acidification another oxidation product, peroxynitrite (*vide infra*), isomerized to nitrate[24]). The neutralized samples were assayed for NO_2^- using a calibration curve for nitrite that was prepared in the presence of RB and nitromethane (Figure 1A). Figure 1B shows the ratio of NO_2^- produced to O_2 photoconsumed as a function of the *aci*-NM concentration.

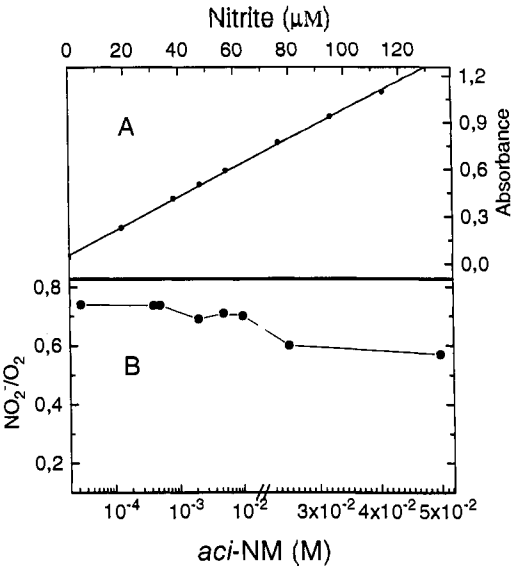

Figure 1. A: Calibration plot for nitrite analysis performed in the presence of RB (25 μM) and nitromethane (25 mM); absorbance of the azo dye was measured at 543 nm in a cell 0.2 cm pathlength. B: Mol ratio of nitrite produced to oxygen consumed during *aci*-NM photooxidation measured for different concentrations of *aci*-NM; analysis was done as described in Experimental Section.

The most accurate analysis occurs at low *aci*-NM concentrations where this ratio is close to 0.75 (Figure 1B).

Production of peroxynitrite was estimated from oxygen recovery catalyzed by copper[24] (50 μM $CuSO_4$) injected into an anaerobic sample after irradiation.

Procedures to detect formaldehyde and methanol are described in the addendum.

Results

We first examined the conditions under which NM occurs in the *aci* form. In aqueous solution, nitromethane takes the form of the *aci* tautomer only at alkaline pH. The aqueous *aci* form absorbance contained a distinctive band at λ_{max} = 240 nm (Figure 2A) whose intensity varied with pH, and whose pK_a (nitro) value was close to the literature value of 10.2 (Figure 2B, plot 1). In 0.25 M NaOH, practically all NM is found in the *aci* form.

Solutions of NM in NaOH (0.5 M) were initially colorless but became yellow-orange after storage in the dark for several hours, with color development noticeably faster in the more concentrated NM solutions (~3 h for 0.1 M solution). These dark processes were accompanied by moderate oxygen consumption at a rate that was a linear function of the NM concentration. From the initial O_2 consumption rates in the dark, we estimate the rate constant to be about 0.87 M^{-1} s^{-1}. This rate decreased by about 20% when the chelating agent DTPA (1 mM) was added to the solution, suggesting that redox active metal cations may be involved. Dark autoxidation in aerobic NaOH solution was also accompanied by the formation of nitrite (not shown). In order to minimize the effect of dark decomposition, alkaline solutions of NM were prepared fresh a few minutes before photochemical experiments, and dark consumption was always subtracted from the photoconsumption rates.

When RB solutions (pH 5 to >12) containing NM were irradiated (λ > 400 nm), oxygen photoconsumption depended on pH. In solutions below pH 7, practically no oxygen photoconsumption was observed, but above pH 9 it increased markedly (Figure 2B, plot 1) in a manner very similar to the increase in absorbance of the *aci*-NM band. The close similarity between the pH-dependence curves for *aci*-NM absorbance and O_2 photoconsumption strongly suggests that *aci*-NM is the main substrate for photooxidation.

(17) Bilski, P.; Chignell, C. F. *Photochem. Photobiol., A: Chem.* **1994**, *77*, 49.
(18) (a) Bilski, P.; Li, A. S. W.; Chignell, C. F. *Photochem. Photobiol.* **1991**, *54*, 345. (b) Bilski, P.; Chignell, C. F. *J. Biochem. Biophys. Methods*, submitted.
(19) Hall, R. D.; Chignell, C. F. *Photochem. Photobiol.* **1987**, *45*, 459.
(20) Battino, R.; Rettich, T. R.; Tominaga, T. *J. Phys. Chem. Ref. Data*, **1983**, *12*, 163.
(21) Khomutov, N. E.; Konnik, E. I. *Russ. J. Phys. Chem.* **1974**, *48*, 359.
(22) *Standard methods of the examination of water and wastewater*, 16th ed.; American Public Health Association: Washington, DC, 1985; p 404.
(23) (a) Nielsen, A. T. In *Nitrones, nitronates and nitroxides*; Patai, S., Rappoport, Z., Eds.; J. Wiley & Sons: New York, 1989; pp 1–139, and references therein. (b) Park, J.-Y.; Lee, Y.-N. *J. Phys. Chem.* **1988**, *92*, 6294.
(24) Plumb, R. C.; Edwards, J. O. *Analyst* **1992**, *117*, 1639.

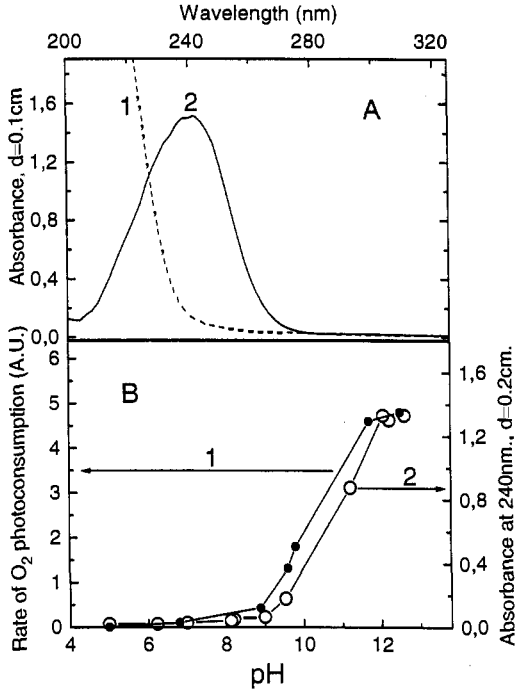

Figure 2. 2. A: Absorption spectra of nitromethane in water ([NM] = 10 mM, spectrum 1, air reference) and in NaOH solution, spectrum 2; extinction coefficient $\epsilon = 7.5 \times 10^3\ M^{-1}\ cm^{-1}$, [NaOH] = 1 M, [NM] = 2 mM, both NaOH solution and NM in H_2O were used as references). B: Absorbance at 240 nm (plot 1) and the rate of oxygen consumption (plot 2) as a function of pH; air saturated solutions contained RB (25 μM), appropriate buffer (0.1 M), and NM (10 mM for oxygen consumption and 1.5 mM for absorbance).

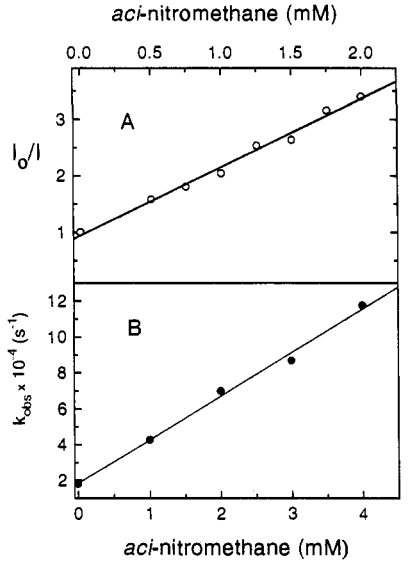

Figure 3. Quenching of $^1O_2$ phosphorescence by NM in NaOD solution (0.2 M) containing RB (25 μM). A: Stern–Volmer plot; B: observed rate constant of $^1O_2$ phosphorescence decay as a function of *aci*-NM concentration.

In deuterated alkaline (NaOD) solutions, the rate of oxygen photoconsumption increased substantially over the rate in NaOH, which suggests a singlet oxygen mechanism. We sought evidence for singlet oxygen involvement in two ways: azide quenching of oxygen photoconsumption, and nitromethane quenching of singlet oxygen phosphorescence. In the former test, the singlet oxygen quencher azide (20 mM) markedly decreased oxygen photoconsumption by NM in NaOH solution. In the latter, *aci*-NM also quenched steady-state and pulse $^1O_2$ phosphorescence generated by Rose Bengal (RB) (Figure 3, parts A and B, respectively). We

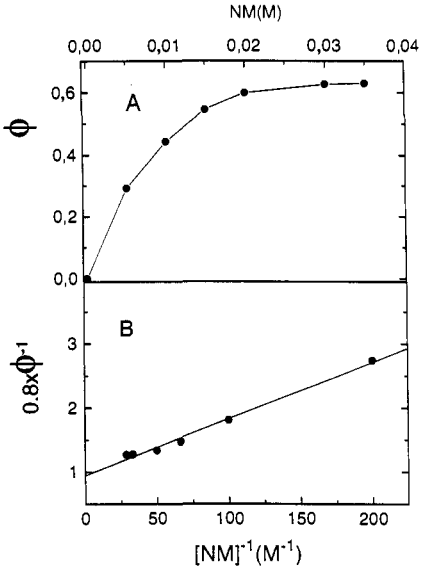

Figure 4. 4. A: The quantum yield of oxygen consumption as a function of nitromethane concentration; air saturated solutions contained RB (25 μM) and NaOH (0.25 M); irradiation was carried out using a glass cutoff filter combination (450 nm) and a neutral density filter attenuating light intensity ca. 60 times. B: plot for eq 2 (reciprocal of ϕ as a function of reciprocal of *aci*-NM concentration).

calculated the phosphorescence quenching rate constant, $k_q = 2.4 \times 10^7\ M^{-1}\ s^{-1}$, taking 54.6 μs as the $^1O_2$ lifetime in D_2O[25] in steady-state experiments. The same quenching value (2.4 ± 0.1) $\times 10^7\ M^{-1}\ s^{-1}$ was obtained from pulse experiments. All these observations support the participation of $^1O_2$ in *aci*-NM oxidation.

The quantum yield of O_2 photoconsumption, $\phi(O_2)$, by *aci*-NM increased with increasing concentration of NM in NaOH solution, reaching a plateau above concentrations of about 20 mM (Figure 4A). (For these calculations, we employed the initial photoconsumption rates to minimize any contribution from oxidation of degradation products which might accumulate in the course of the reaction (*vide infra*)). We used this concentration dependence to measure the chemical contribution to $^1O_2$ quenching as follows.

Singlet oxygen can be quenched chemically or physically or it can decay spontaneously (reactions 1–3 below, respectively).

$$^1O_2 + CH_2{=}NO_2^- \xrightarrow{k_c} \text{products (HCOOH, } NO_2^-) \qquad \text{(R.1)}$$

$$^1O_2 + CH_2{=}NO_2^- \xrightarrow{k_p} O_2 + CH_2{=}NO_2^- \qquad \text{(R.2)}$$

$$^1O_2 \xrightarrow{k_d} O_2 \qquad \text{(R.3)}$$

Equation 1 which defines the rate of $^1O_2$ production can be combined with the rate constants for reactions 1–3 for $^1O_2$ decay, and that under a steady-state approximation leads to eq 2 below.

$$d[^1O_2]/dt = K \qquad \text{(eq 1)}$$

$$0.8/\phi = (k_c + k_p)/k_c + k_d/k_c \times [NM]^{-1} \qquad \text{(eq 2)}$$

The left-hand side of eq 2 was obtained from eq 1 and the quantum yield of oxygen consumption, defined as $\phi = \{-d[O_2]/dt\}/0.8K$, where 0.8 is the quantum yield of $^1O_2$ sensitization by the RB triplet. The spontaneous decay rate k_d for $^1O_2$ in water is $2.3 \times 10^5\ s^{-1}$, and the triplet state in RB is formed with near 100% efficiency.[26]

(25) The $^1O_2$ lifetime in basic D_2O solution has been measured using the apparatus described in the Experimental Section.

Scheme 1

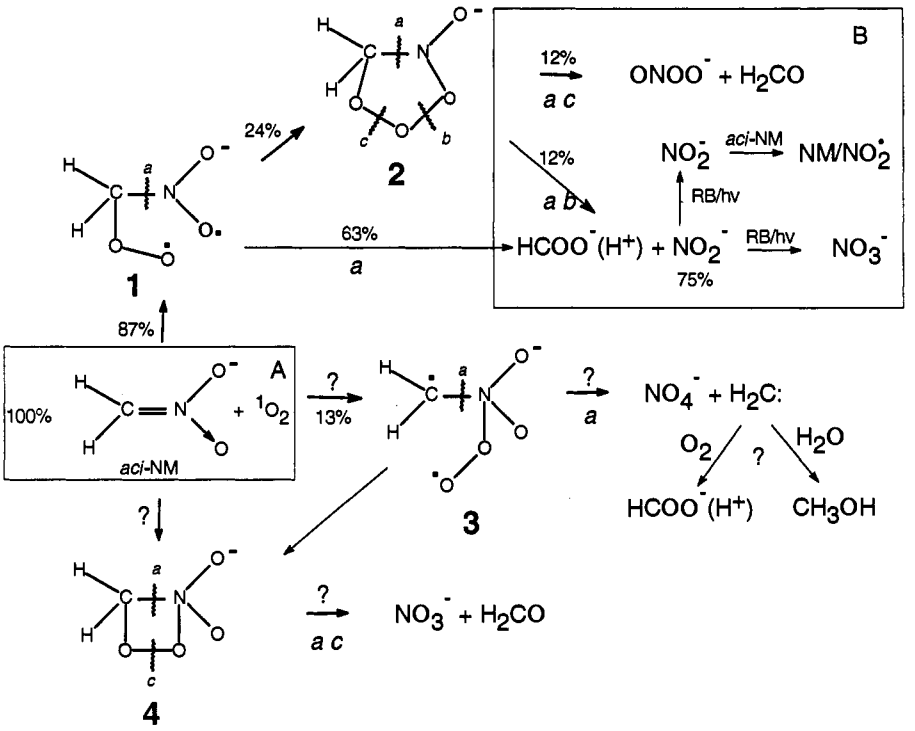

Equation 2 predicts a linear relationship between ϕ^{-1} and $[NM]^{-1}$, and a plot of the data (Figure 4B) does indeed produce a straight line. The slope (k_d/k_c) was used to calculate a chemical quenching rate constant $k_c = 2.6 \times 10^7$ M^{-1} s^{-1}. The intercept ($(k_c + k_p)/k_c$) is close to unity,[27a] which means that the value of the rate constant for physical quenching, k_p, is small compared to k_c. The k_c value obtained from oxygen consumption measurements is very similar to the $k_q = (k_c + k_p)$ value calculated from $^1O_2$ phosphorescence quenching ($k_q = 2.4 \times 10^7$ M^{-1} s^{-1}, *vide supra*). Considering that completely different methods were used for the evaluation of the rate constants, the agreement is quite satisfactory.

The high rate constant for the chemical quenching of $^1O_2$ by *aci*-NM and the resultant rapid oxygen consumption indicate that oxidation products must be formed efficiently. These products must originate from a transient intermediate(s) formed by the addition of $^1O_2$ to *aci*-NM.[27b] The exclusively chemical quenching also means that the initial stoichiometry of oxygen consumed to NM oxidized must be 1:1. Four possible initial peroxy intermediates (**1–4**) are shown in Scheme 1, together with putative decomposition pathways.

To characterize by EPR the immediate decomposition products of the *aci*-NM-O_2 peroxy transient(s), we used another spin trap, 5,5-dimethyl-1-pyrroline *N*-oxide (DMPO) in a nontraditional[27c] way as follows: *Aci*-NM is known to undergo nucleophilic addition to DMPO[28] forming a hydroxylamine, DMPOH/CH=NO_2^- (**5**), (Scheme 2). If the photochemistry of the *aci*-NM moiety in the adduct is the same as in free *aci*-NM then it should be possible to identify the photoproduct(s) by oxidation of **5** to the corresponding nitroxide radical (**6**) (Scheme 2). It is known that the hydroxylamine moiety is oxidized/photooxidized to nitroxide under conditions used in our present experiments.[29] We used this novel approach to obtain "DMPO-labeled" fragments from the cleavage of *aci*-nitro moiety (**7**) during its oxidation forming **8** (Scheme 2).

The formation of the hydroxylamine **5** in our system was proved as follows: When DMPO and NM were added to nonchelated NaOH solution, an EPR spectrum was generated that was typical of a carbon-centered adduct, DMPO/R•. The signal was observed in the dark, and grew in intensity (Figure 5A) but was absent when *aci*-NM was omitted. The EPR signal could be completely inhibited by addition of 0.5 mM DTPA (Figure 5B), which suggests that redox active metal ions might be involved in the production of this radical. This behavior is characteristic of the hydroxylamine moiety[29] and confirms that *aci*-NM reacted with DMPO by nucleophilic addition (Scheme 2).

Irradiation of the RB solution containing DMPOH/CH=NO_2^- resulted in the EPR spectra shown in Figure 6. Spectrum A, which was recorded during the first 4 min of exposure, contains contributions from three species, identified as DMPO/$CO_2^{\bullet-}$, DMPO/R• and DMPO/OH•.[30a] (Identification of all radical adducts was based on the values of the hfsc's, Table 1). The DMPO/$CO_2^{\bullet-}$ adduct (marked with asterisks in Figure 6, parts A and B) was formed rapidly[30b] but also disappeared quickly during irradiation.[30c] The second carbon-centered adduct, DMPO/R•, has the same splitting values as the radical formed in the dark process (*vide supra*). Most likely, both $^1O_2$ and RB triplet participated in hydroxylamine to nitroxide oxidation,[29] in addition to the dark oxidation catalyzed by metal ions (*vide supra*).

Upon continued irradiation of this solution, a fourth species slowly accumulated (Figure 6C) and finally became dominant (Figure 6D). The hfsc's of this species are characteristic of the $^-O_2\dot{N}CHNO_2^-$ radical adduct.[2-4] This adduct is formed by addition of $NO_2^{\bullet}$ to *aci*-NM to give $^{-\bullet}O_2NCH_2NO_2^-$ followed by

(26) Murasecco-Suardi, P.; Gassmann, E.; Braun, A. M.; Oliveros, E. *Helv. Chim. Acta* **1987**, *70*, 1760.

(27) (a) Separating $^1O_2$ physical quenching by *aci*-NM is of low accuracy because intercept value (Figure 4B) is sensitive to experimental errors. In addition, a small contribution of the RB triplet quenching by *aci*-NM may interfere with $^1O_2$ sensitization, especially at higher NM concentrations. This is suggested by the EPR signal of the reduced RB radical anion that we detected in aerobic solution containing 50 mM *aci*-NM amd 50 μM RB. (b) A less likely possibility, a minor contribution to $^1O_2$ quenching *via* electron transfer from *aci*-NM to $^1O_2$, cannot be entirely excluded. However, such a process would produce superoxide and ultimately H_2O_2, which were not detected. (c) DMPO is a well known and widely used spin trap for the identification of free radicals. In its traditional use, the addition of free radical to DMPO produces a more stable radical, the so-called DMPO radical adduct, readily detectable by EPR.

(28) Bonnett, R.; Brown, R. F. C.; Clark, V. M.; Sutherland, I. O.; Sir Todd, A. *J. Chem. Soc.* **1959**, 2094.

(29) Bilski, P.; Motten, A. G.; Bilska, M.; Chignell, C. F. *Photochem. Photobiol.* **1993**, *58*, 11.

Scheme 2

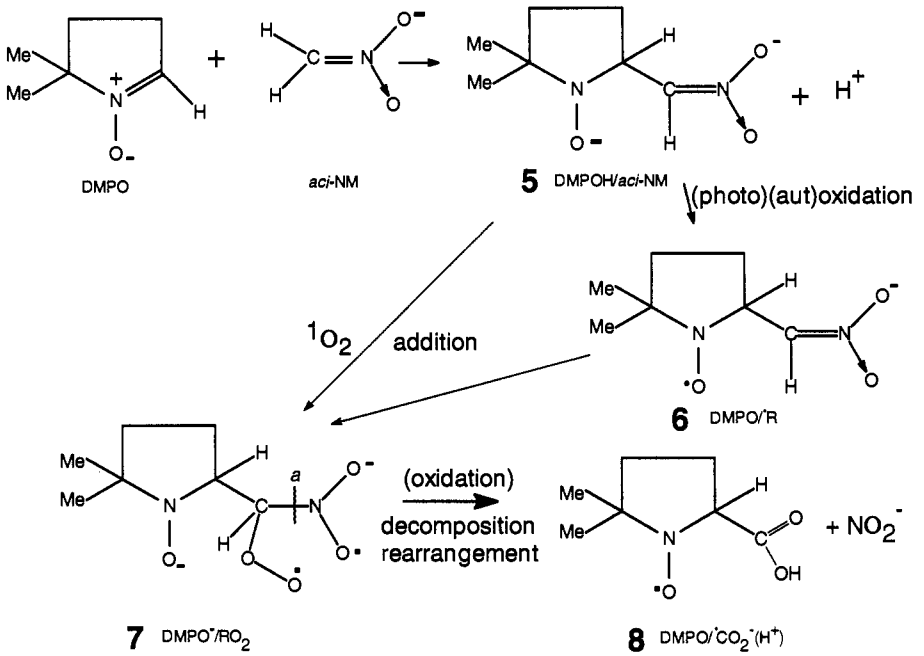

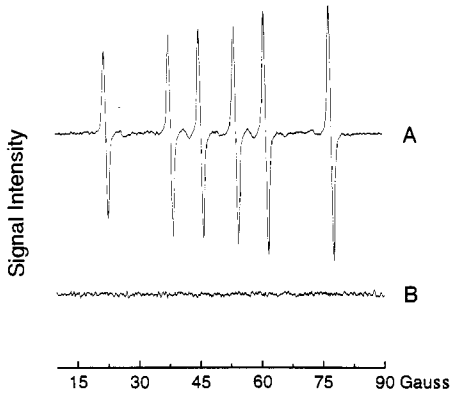

Figure 5. 5. (A) EPR spectrum of DMPO/CH=$NO_2^{\bullet-}$ produced in a system consisting of DMPO (40 mM) and NM (9 mM) in NaOH solution (0.2 M) in the dark. (B) Same as A but in the presence of DTPA (0.5 mM). The radical in A is produced by nucleophilic addition of *aci*-NM to DMPO followed by autooxidation of the resultant hydroxylamine. Experiment B shows that the process is dependent on the presence of redox-active metal ions. Instrumental settings: microwave power 20 mW; modulation amplitude 0.33 G; gain 1×10^3; time constant 0.25 s; scan rate 4 min.

the dissociation of one βH at high pH. Irradiation of the solution in which DMPO was omitted also generated the NM/$NO_2^{\bullet}$ adduct (Figure 7B). As in previous experiments, this signal was not present initially but appeared after several minutes of exposure and then grew slowly during irradiation. It was completely inhibited by azide (Figure 7C), indicating that $^1O_2$ is involved.[31]

Formate is a stable molecule so that it should also accumulate in the absence of DMPO, which was confirmed as follows. A sample containing NM (50 mM) and RB (50 μM) at pH 12 was irradiated for 20 min with continuous O_2 bubbling and then neutralized to pH ca. 7, and DMPO (50 mM) and H_2O_2 (100 mM) were added.[32a] The resulting EPR spectrum contained the DMPO/HO$^{\bullet}$ and DMPO/$CO_2^{\bullet-}$ adducts based on the hfc (Figure 8A). The DMPO/$CO_2^{\bullet-}$ adduct was not observed if the same procedure was applied to a nonirradiated sample (Figure 8B). Thus HCOOH is produced even when *aci*-NM oxidation is carried out in the absence of DMPO, which confirms that the *aci*-nitro moiety in both *aci*-NM and DMPOH/CH=NO_2^- may undergo similar degradation processes.

The generation of nitrite during *aci*-NM photooxidation was assayed spectrophotometrically (Figure 1B). Approximately 75% of the photoconsumed oxygen (based on initial consumption kinetics) is reflected in nitrite production. We determined that the concentration of nitrite was not decreased by its photosensitized oxidation: in a control experiment, oxygen photoconsumption by nitrite ([NO_2^-] < 0.1 mM) was negligible compared to that of *aci*-NM.[32b]

We estimated the concentration of peroxynitrite ($ONOO^-$) by measuring the oxygen released by Cu^{2+} addition[24] immediately after irradiation was stopped. Peroxynitrite is more stable in alkaline solutions which facilitates its accumulation,[24] and $ONOO^-$ is known to decompose[24] releasing O_2 in the presence of Cu^{2+}. Oxygen recovery, relative to photoconsumed oxygen, was 1, 3.8,

(30) (a) The traces of DMPO/OH$^{\bullet}$ adduct are formed from the oxidation of DMPO by singlet oxygen as was shown by Feix, J. B.; Kalyanaraman, B. *Arch. Biochem. Biophys.* **1991**, *291*, 43. (b) Observation of the DMPO/$CO_2^{\bullet-}$ signal at the early stage of the photoprocess demonstrates that the DMPO/$CO_2^{\bullet-}$ is the immediate decomposition product of the peroxide transient (DMPO˙/RO_2 in Scheme 2). The DMPO/$CO_2^{\bullet-}$ adduct cannot be produced by traditional trapping of $CO_2^{\bullet}$ by DMPO because no formate was present when irradiation started; moreover, formate cannot be oxidized by $^1O_2$ and the RB triplet. The signal intensity we observed in the first scan (Figure 6A) was stronger compared to that when formate was accumulated (after 20 min of irradiation[32a]) and the sample was treated with 0.1 M H_2O_2 (Figure 7). (c) The rapid decay was caused by the short lifetime of this radical in our photochemical system and because radical production decreased due to oxygen depletion during irradiation.

(31) The irradiation of RB with *aci*-NM in anaerobic solution hardly produced any signal of the NM/$NO_2^{\bullet}$ adduct, even though the EPR signal from the reduced dye ($RB^{\bullet-}$) was observed.[27a]

(32) (a) The traces of redox active cations (e.g. present from nonchelated phosphate buffer) were sufficient for the Fenton reaction which produces the hydroxyl radical HO$^{\bullet}$. DMPO is known to trap the HO$^{\bullet}$ radical which oxidizes formate producing the formyl radical, which was also trapped by DMPO (Figure 8A, asterisks). In this experiment DMPO was used as a spin trapping agent in the traditional way. (b) Nitrite concentration for the control experiment was estimated assuming a yield of unity in air saturated water when 30% of oxygen was consumed. Nitrite concentration can be additionally decreased somewhat if peroxynitrate (NO_4^-) is produced from the decomposition of the initial peroxide(s) (Scheme 1), because NO_4^- may oxidize NO_2^- to nitrate. (c) Formaldehyde production must be minor in our system. However, the formyl moiety was the main product when 1-nitromethyl)alkylphosphonate was oxidized by $^1O_2$ in basic methanol at low temperature:[16b] the aldehyde yield increased with decreasing temperature (to −78 °C), and the reaction was used to prepare (1-formylalkyl)phosphonates.[16b] A similar reaction was used to prepare other carbonyls from nitronate salts.[16a] In our experiments, the higher temperature (25 °C) and solvent polarity evidently caused the transient biradical produced by $^1O_2$ addition to *aci*-NM to readily decompose to thermodynamically stable products rather than forming cyclic the 1,2 adduct transient that was postulated as an intermediate for the above reaction.[16b]

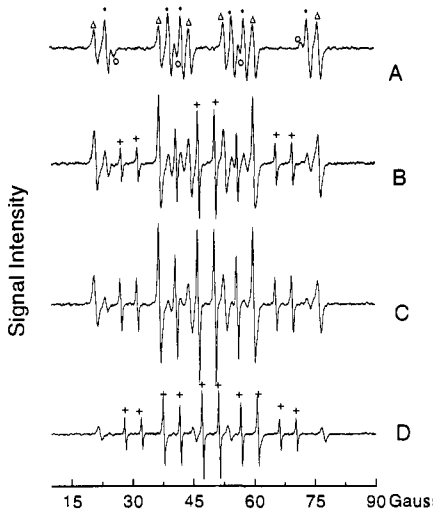

Figure 6. 6. EPR spectra observed during irradiation of RB (50 μM), DMPO (40 mM), and NM (9 mM) in the presence of DTPA in a NaOH solution (0.2 M). (A) First scan (0–4 min); three radical species are present: DMPO/$CO_2^{\bullet-}$ (*), DMPO/$CHNO_2^{\bullet-}$ (Δ), and DMPO/HO$^\bullet$ (O). (B) Second scan; DMPO/$CO_2^{\bullet-}$ and DMPO/HO$^\bullet$ are decaying while NM/$NO_2^\bullet$ (+) is formed. (C and D) Third and forth scans, respectively, showing gradual accumulation of the NM/$NO_2^\bullet$ radical, which becomes a dominating species (D).

Table 1. Hyperfine Splitting Constants (Gauss) from EPR Spectra of DMPO and NM Radical Adducts Observed in Photochemical and "Dark" Processes

radical adduct	production	a_N	a_H
NM/$NO_2^\bullet$	photochemical in NaOH	9.67 (2N)	4.14 (1H)
DMPO/R$^\bullet$	"dark" and photochemical in NaOH	16.08	23.57
DMPO/$CO_2^{\bullet-}$	photochemical in NaOH, and using H_2O_2 at pH 7	15.83	18.79
DMPO/HO$^\bullet$	using H_2O_2 at pH 7	14.9	14.9
DMPO/HO$^\bullet$	photochemical in NaOH	16.01	15.63

and 6% at pH 8.7, 9.7, and in 0.5 M NaOH solution, respectively. Stoichiometrically, the concentration of peroxynitrite is expected to be twice as high as the concentration of released oxygen ($ONOO^- \rightarrow NO_2^- + {}^1/_2O_2$).

Production of peroxynitrite requires that formaldehyde is also formed (Scheme 1, box B). However, no formaldehyde was detected using a sensitive HPLC assay. It is possible that the high reactivity of formaldehyde in alkaline solution, especially *in statu nascendi*, may have prevented the detection of low H_2CO concentrations.[32c]

To determine whether the oxidation products of *aci*-NM could be photooxidized further, we measured the stoichiometry of photoconsumed O_2 vs oxidized NM during prolonged irradiation (~0.5 h). Oxygen concentration decreased by 0.73 mM during the complete oxidation of NM (0.5 mM), which gives a ratio of photoconsumed oxygen to oxidized NM of ca. 1.4. This ratio may still contain a contribution due to RB photodegradation in the presence of *aci*-NM, which could not be adjusted in a control O_2 consumption experiment. However, the ratio is clearly higher than 1, suggesting that the initial degradation product, possibly nitrite, is further oxidized to nitrate. In support of this, nitrate was detected using copperized cadmium[22] granules for the reduction of nitrate to nitrite.[33]

Discussion

Our results show that the *aci*, but not the nitro, form of NM interacts with $^1O_2$. While the >C=N double bond in the *aci* tautomer is undoubtedly involved in this interaction, the negative charge carried by the *aci*-NM molecule is important for the observed quenching rate constant, $k_q = 2.4 \times 10^7$ M^{-1} s^{-1}. Unconjugated double bonds in uncharged molecules show much lower quenching efficacies,[34] e.g. >C=N bonds in oximes quench $^1O_2$ (mostly *via* 1,2 addition) with rate constants no higher than 10^5 M^{-1} s^{-1}.

The chemical quenching of $^1O_2$ by *aci*-NM implies that at least four different peroxy intermediates, **1–4** (Scheme 1), should be considered as possible primary products. However, based on the detected products and the reactions we measured directly (boxes A and B in Scheme 1), transients **1** and **2** appear to predominate. We postulate that the major transient is the biradical peroxide **1** produced when $^1O_2$ adds to the carbon atom of the *aci*-NM molecule. This biradical may decompose (*vide infra*) or rearrange by intramolecular recombination to an ozonide[35] **2**. Such an ozonide is unlikely to be produced directly *via* the 1,3 addition of $^1O_2$, because the oxygen atom in *aci*-NM molecule (site 3 for bond formation) does not have any radical density prior to the breaking of the double C–N bond.

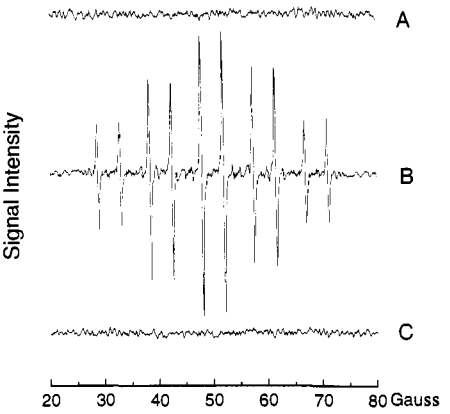

Figure 7. EPR spectra observed during irradiation of RB (50 μM) and NM (9 mM) in aerated NaOH solution (0.2 M). (A) Dark, prior to exposure. (B) During irradiation; signal of the NM/$NO_2^\bullet$ radical is observed. (C) Same as B but in the presence of a singlet oxygen quencher, sodium azide (20 mM). Instrumental settings: same as in Figure 5, except gain, 2×10^4.

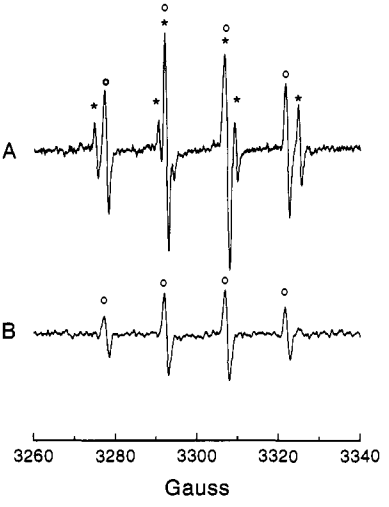

Figure 8. 8. (A) EPR spectra of DMPO/$CO_2^{\bullet-}$ (*) and DMPO/HO$^\bullet$ (O) observed in the dark from a photoirradiated sample consisting of RB (50 μM) and NM (60 mM) in an O_2-saturated NaOH. (0.2 M). Following the photolysis the sample was acidified pH ca. 7, and DMPO (100 mM) and H_2O_2 (30 mM) were added. (B) Same as A prior to photolysis. Instrumental settings: same as in Figure 5, except gain, 2×10^4.

(33) Under conditions used for nitrate reduction, this form of cadmium also reduced nitromethane to nitrite. Therefore this sensitive method for nitrate assay could not be used routinely for all samples unless all nitromethane had been previously consumed and most of nitrite was photooxidized to nitrate.

(34) Wilkinson, F.; Brummer, J. G. *J. Phys. Chem. Ref. Data* **1981**, *10*, 809.

Ozonide intermediacy is clearly indicated by the presence of peroxynitrite[36] which cannot be generated in our system by other transients (Scheme 1). In contrast, nitrite and formate are common decomposition products of transients **1** and **2**. Nitrite is produced directly by cleavage *a* in **1**, or *a* and *b* in **2** (Scheme 1). Formate must be formed *via* a putative intermediate $H_2\dot{C}OO^{\bullet}$, generated concomitantly with nitrite and rearranging to $HCOO^-(H^+)$, Scheme 1. Quantitation of nitrite and peroxynitrite appeared useful to determine which precursor, biradical **1** or ozonide **2**, contributes more to the observed product concentrations. Decomposition of the ozonide should give equal amounts of $HCOOH/NO_2^-$ and $H_2CO/OONO^-$ (box B, Scheme 1), assuming the same probability of breaking either O—O bond (c or b in **2**) concomitantly with the C—N bond cleavage (a in **2**). Thus, the 12% concentration of peroxynitrite, derived from 6% O_2 release, sets a likely range for the total ozonide intermediacy at 24%.

If **2** decomposes with the same probability along paths *ac* and *ab* (Scheme 1), then 12% of nitrite, from the total 75% assayed, may be formed *via* the ozonide. We believe that the remaining part, ca. 63% (75% − 12%), originates mostly from direct decomposition of **1**. From its structure, **1** appears to be an unstable species that would more readily decompose to stable products than undergo cyclization (*vide infra*). Therefore, about 87% (63% + 24%) of $^1O_2$ that initiates *aci*-NM oxidation adds to the carbon atom of *aci*-NM forming the biradical **1**.

About 13% (100% − 87%) of $^1O_2$ is used in unknown minor processes which were difficult to verify and are addressed as mere possibilities (marked with "?" in Scheme 1). The well-known 1,2 addition of $^1O_2$ to a double bond would form peroxy transient **4**. The most likely decomposition of **4** is along the *ac* path forming nitrate and formaldehyde (Scheme 1), which excludes efficient formation of nitrite.[38] We believe that the formation of transient **4** in our system is a minor process, which may be due to slower $^1O_2$ quenching *via* pure 1,2 addition ($k_q \approx 10^5\ M^{-1}s^{-1}$) compared to that observed for *aci*-NM ($k_q \approx 10^7\ M^{-1}\ s^{-1}$). The formation of the strained four-membered ring in **4** must also compete unfavorably with other faster decomposition paths at room temperature.

A minor fraction of $^1O_2$ may also add to the nitrogen atom in the *aci*-NM molecule forming transient **3** which decomposes to peroxynitrate (NO_4^-) and methylene carbene, $:CH_2$, (to satisfy stoichiometry). Peroxynitrate is a known species[39-41] and may form during the oxidation of nitrite by singlet oxygen;[42] NO_4^- is strongly oxidative[41] and may react fast in our system, if produced. Carbenes are also a highly unstable species[43] and are known to react with many molecules, including oxygen[43] (the reaction of $:CH_2$ with O_2 would produce formic acid). Our attempts to detect methanol from a potential carbene hydrolysis ($:CH_2 + H_2O \rightarrow CH_3OH$) were unsuccessful. Thus, we cannot account for the reactions started by ca. 13% of $^1O_2$ because products other than nitrite, peroxynitrite, and formate are produced at low concentrations, and there are no sensitive analytical methods for their analysis.

During prolonged irradiation, O_2 consumption exceeded stoichiometric NM decomposition predicted by the reaction in box A, Scheme 1. This is probably attributable to nitrite photooxidation since nitrite is the main product that is prone to photooxidation by RB[44] and eosine[42] leading to O_2 consumption. During nitrite photooxidation, the $NO_2^{\bullet}$ free radical is produced (box B, Scheme 1) and then trapped by *aci*-NM yielding the $NM/NO_2^{\bullet}$ radical adduct (Figure 7). That the $NM/NO_2^{\bullet}$ adduct was not observed when irradiation started, but only appeared after several minutes of irradiation when NO_2^- had accumulated, supports the possibility that $NO_2^{\bullet}$ is produced *via* nitrite photooxidation. Thus, the possibility that the $NM/NO_2^{\bullet}$ radical adduct may be photochemically produced *via aci*-NM photooxidation must be considered when *aci*-NM is used as a spin trap, especially for $NO_2^{\bullet}$, in the presence of singlet oxygen.

Another aspect of our study which deserves some comment is a novel use of DMPO to obtain "DMPO-labeled" formic fragment **8** from the photooxidation of *aci*-nitro moiety by $^1O_2$. Formate is a stable molecule and its accumulation after prolonged irradiation could be due to secondary oxidation reactions (e.g. the oxidation of formaldehyde). By using DMPO to "label" the decomposition fragment we have identified formate as a primary decomposition product. In addition, the $^1O_2$ oxidation of DMPOH/*aci*-NM nucleophilic adduct and *aci*-NM suggests that the oxidations of other *aci*-nitro compounds may occur by the same comparable mechanism.

In conclusion, singlet oxygen reacts rapidly with *aci*-NM initiating the efficient decomposition of the *aci*-nitro moiety *via* peroxy transients and nitrogen peroxide(s). Nitrite and formate are the main oxidation products, and peroxynitrite is a minor one. Such products indicate that $^1O_2$ adds mainly to the carbon atom of the *aci*-NM molecule, and the resultant biradical decomposes fast in competition with cyclization to ozonide intermediate.

Addendum

HPLC Analysis of Formaldehyde. The solutions containing RB (50 μM) and NM (30 mM) at pH 9, 11, and 12 were irradiated for 15–60 min with slow continuous O_2 bubbling. In such prepared samples, formaldehyde was analyzed as the corresponding 2,4-dinitrophenylhydrazone by the procedure of Barone and Walter[45] using a C_{18}-Bondapack column (3.9 mm × 300 mm) eluted isocratically with water/CH_3CN/tetrahydrofuran (60:60:10; v/v/v) at a flow rate of 1 mL/min. Detection was by absorbance at 360 nm. No formaldehyde was detected in the irradiated samples.

GC Analysis of Methanol. Sample irradiation for methanol detection was analogous to that for the formaldehyde analysis, except that a distillate from the irradiated solution was injected into a GC column. Methanol was analyzed on a Varian 1400 GC using 4 ft × 1/8 in. SS column Porapak QS at constant temperature 100 °C using 4 μL injections. Helium flow was 25 mL/min. Methanol/water mixture (30 μg/mL) was used as a calibration standard, and methanol detectability was 5 μg/mL. No methanol was detected in distillate.

Acknowledgment. Authors thank Dr. Phillip Albro and Dr. Carol Parker for the HPLC and MS analysis of methanol and Mr. Robert H. Sik for the HPLC analysis of formaldehyde and appreciate helpful discussion with Dr. Ann G. Motten.

(35) (a) Similar ozonides are thought to be formed during the reaction of compounds containing nitrogen–carbon double bonds with ozone.[35b] An ozonide-like transient was also postulated for the reaction of $^1O_2$ with some nitrones in CH_2Cl_2 at low temperature.[35c] (b) Bailey, P. S. In *Ozonation in organic chemistry*; Academic Press: New York, 1978; Vol. I, pp 225–453, and references therein. (c) Ching, T.; Foote, C. S. *Tetrahedron Lett.* **1975**, 3771.

(36) Peroxynitrite anion can isomerize to nitrate or decompose releasing oxygen. Isomerization/decomposition decreases rapidly on going to alkaline solution where $ONOO^-$ was found to be quite stable ($k_{iso} = 10^{-4}\ s^{-1}$ at pH 10).[24] Peroxynitrite is a strong oxidizer.[37]

(37) Koppenol, W. H.; Moreno, J. J.; Pryor, W. A.; Ischiropoulos, H.; Beckman, J. S. *Chem. Res. Toxicol.* **1992**, *5*, 834–842.

(38) Theoretically, transient **4** could also decompose to nitrite. This would require, however, preferential cleavage of the N—O bond in the ring in **4**. This may mean that the N—O bond was weak, therefore unlikely to be formed, in the first place, which points back to **1** as the main nitrite precursor.

(39) Howard, C. J. *J. Chem. Phys.* **1977**, *67*, 5258.

(40) Kenley, R. A.; Trevor, P. L.; Bosco, B. Y. *J. Am. Chem. Soc.* **1981**, *103*, 220.

(41) Løgager, T.; Sehested, K. *J. Phys. Chem.* **1993**, *97*, 10047.

(42) Bilski, P.; Szychliński, J.; Oleksy, E. *Photochem. Photobiol., A: Chem.* **1988**, *45*, 269.

(43) Scaiano, J. C. In *Handbook of organic photochemistry*; Scaiano, J. C., Ed.; CRC Press Inc.: Boca Raton, FL, 1989; Vol. II, p 211, and references therein.

(44) Bilski, P.; Motten, A. G.; Chignell, C. F.; Szychlinski, J.; Oleksy, E. *Photochem. Photobiol.* **1990**, *51S*, 5S.

(45) Barone, J. P.; Walter, T. H. *Waters Column*, Autumn 1991, 1.